**Left ventricular mechanical and energetic changes in long-term isoproterenol-induced hypertrophied hearts of SERCA2a transgenic rats**

Shinichi Mitsuyama[1,a], Daisuke Takeshita[1,a], Koji Obata[1,a], Guo-Xing Zhang[1,2], Miyako Takaki[1]

[1]Department of Physiology II, Nara Medical University School of Medicine, 840 Shijo-cho, Kashihara, Nara 634-8521, Japan

[2]Department of Physiology, Medical College of Soochow University, Dushu Lake Campus, Suzhou Industrial Park, Suzhou 215123, P.R. China

[a]These authors contributed equally to this work.

Author contributions:

Miyako Takaki designed and supervised the present study. Shinichi Mitsuyama, Daisuke Takeshita, Koji Obata and Miyako Takaki conducted experiments and obtained the data. Koji Obata and Guo-Xing Zhang established the transgenic rats. Shinichi Mitsuyama and Miyako Takaki analyzed the data and drafted the manuscript.

Running Head: Cardiac hypertrophy in SERCA2a transgenic rats

Corresponding author: Prof. Miyako Takaki, Ph.D.

Departments of Physiology II and Molecular Pathology, Nara Medical University School of Medicine, 840 Shijo-cho, Kashihara, Nara 634-8521, Japan

Email: mtakaki@naramed-u.ac.jp, Tel: +81-744-29-8829, Fax: +81-744-23-4696

**Abstract**

Overexpression of cardiac sarcoplasmic reticulum $Ca^{2+}$-ATPase (SERCA2a) has been suggested as a strategic intervention for cardiac failure. However, its benefit in wild-type (WT) rats with normal SERCA2a levels seems to be small. To investigate whether it would be beneficial in a cardiac failure model with down-regulated SERCA2a levels, we made a cardiac hypertrophy model using isoproterenol infusion (1.2 mg $kg^{-1}$ $day^{-1}$ for 1 or 4 weeks; TG-ISO1w and TG-ISO4w, respectively) in SERCA2a transgenic (TG) rats and compared these rats with littermate WT rats that underwent the same treatments (WT-ISO1w and WT-ISO4w). We analyzed the left ventricular (LV) mechanoenergetics in the excised heart using our original cross-circulation system. The downward shift of curvilinear LV end-systolic pressure-volume relations (ESPVRs) observed in WT-ISO4w rats was abolished in TG-ISO4w rats. The slope and $VO_2$ intercept of the $VO_2$ (myocardial oxygen consumption per beat)-PVA (systolic pressure-volume area: total mechanical energy per beat) linear relation did not differ in any of the groups. The most important finding was a significantly smaller $O_2$ cost of LV contractility in the TG-ISO4w group, which means that less $O_2$ is needed to exert the same LV contractility, compared with the other groups. The increased ratio of SERCA2a/phospholamban returned to the level of the WT-control group only in the TG-ISO4w group. Longer-term up-regulation of mitochondrial transcription factor A for genes of mitochondrial enzymes producing ATP was observed in TG rats. In conclusion, longer-term overexpression of SERCA2a will be beneficial in the present cardiac failure model with down-regulated SERCA2a levels.

**Key words:** heart failure, $Ca^{2+}$ handling, oxygen consumption, excitation-contraction coupling

## 1. Introduction

Heart failure is one of the major causes of mortality and morbidity. It can be the result of various diseases, and cardiac hypertrophy is a major risk factor for the development of heart failure. Hypertrophy initially compensates for a lack of cardiac function but ultimately leads to heart failure [1]. Meanwhile, calcium ($Ca^{2+}$) handling is closely related to the contraction-relaxation cycle of the myocardium and to cardiac function [2, 3]. Cardiac sarcoplasmic reticulum $Ca^{2+}$-ATPase (SERCA2a) plays a key role in $Ca^{2+}$ homeostasis [2]. Cardiac dysfunction is related to defective sarcoplasmic reticulum $Ca^{2+}$ uptake caused by a SERCA2a deficiency [2, 4-6]. Accordingly, overexpression of SERCA2a has been suggested as a strategic therapeutic approach for heart failure, and many studies have been reported on its use [4, 6-15].

Previous reports have shown improved myocardial function and improved energetic consumption as a result of a gene transfer of SERCA2a under short-term conditions [8, 9, 12, 13]. However, one report showed that excessive SERCA1a expression caused a decrease in myocyte shortening in normal rabbit hearts [14]. The effect of a high basal level of SERCA2a has been assessed using transgenic SERCA2a-overexpressing rodents [7, 10, 11, 15-17]. However, little is known about the effects of a high basal SERCA2a level on whole-heart mechanics and energetics, and there have been no detailed quantitative analyses of changes in $Ca^{2+}$ handling in excitation-contraction (E-C) coupling at a whole-heart level.

To assess the effect of longer-term overexpression of SERCA2a, we recently established SERCA2a transgenic Wistar rats and evaluated the left ventricular (LV) mechanics and energetics in an excised, blood-perfused whole-heart preparation with a cross-circulation system [18]. This system is designed to perform detailed quantitative analyses of changes in the efficiency of cross-bridge cycling and $Ca^{2+}$ handling in E-C coupling at a whole-heart level through indirect measurements [19]. However, there were no distinct beneficial effects on LV mechanics or energetics in normal SERCA2a transgenic rats, although the tolerance to high $Ca^{2+}$ was greater than that found in normal littermate wild-type rats [18].

The aim of the present study was to investigate whether longer-term SERCA2a overexpression would be beneficial in a cardiac failure model with down-regulated SERCA2a

levels [20]. We previously analyzed a short-term (3 days and 1 week) isoproterenol-induced cardiac compensatory hypertrophy model in normal Wistar rats [21]. In this short-term hypertrophy model, changes in LV mechanical work and energetics were minimal [21]. and analyzed LV mechanics and energetics (various kinds of oxygen consumption, such as consumption for $Ca^{2+}$ handling) for LV contraction and relaxation in these models by using our original cross-circulation system. The functioning of an ATPase such as SERCA2a is highly dependent on the supply of ATP. Therefore, ATP production in mitochondria is closely related to $Ca^{2+}$ handling in cardiac function [22].

## 2. Methods

This investigation conformed to the "Guide for the Care and Use of Laboratory Animals" published by the National Institutes of Health (NIH Publication No. 85-23, revised 1996) and was approved by the Animal Care and Use Committee of Nara Medical University.

### *2.1. Animal models*

We established a strain of SERCA2a-overexpressing transgenic (TG) Wistar rats as previously reported in detail [15, 18]. Male littermate wild-type (WT) Wistar rats (n = 27) and male TG rats (n = 21) weighing 325 ± 38 g to 403 ± 26 g (Table 1) approximately 12 weeks in age were used in the present study. Each group was randomly divided into 3 subgroups: vehicle group (control), 1-week isoproterenol (ISO)-infused group (ISO1w) and 4-week ISO-infused group (ISO4w). ISO (1.2 mg $kg^{-1}day^{-1}$ for 1 or 4 weeks) was subcutaneously administered using an osmotic minipump (model 1003D or 2001, Alzet; Durect, Cupertino, CA) implanted in the neck under pentobarbital sodium (50 mg $kg^{-1}$ ip) anesthesia. Each osmotic minipump was removed more than 2 h before the experiment as previously reported [21, 23].

### *2.2. Echocardiography*

Transthoracic echocardiography was performed for each of the 6 groups. In the ISO-infused groups, the measurement was performed 2 h after the removal of the osmotic minipump [20]. The following parameters were measured and calculated using an Aplio SSA-700A (Toshiba, Tokyo, Japan) equipped with a 12-MHz ultrasound probe (PLT-1202S) under light sedation: LV internal dimensions at systole and diastole (LVIDs and LVIDd, respectively), interventricular septum

thickness at diastole (IVSTd), LV posterior wall thickness at diastole (LVPWTd), LV ejection fraction (EF), and LV fractional shortening (FS). M-mode recordings were performed at the level of the papillary muscles.

*2.3. Surgical preparation*

Analyses of LV mechanoenergetics were performed on the excised cross-circulated heart preparations as reported previously [19]. In each experiment, we used 3 rats: one WT or TG rat was used as a heart donor, and 2 retired breeder male Wistar rats weighing 450–650 g were used as blood supplier and metabolic supporter rats, respectively. All rats were anesthetized with pentobarbital sodium (50 mg $kg^{-1}$ ip), intubated, ventilated, and heparinized (1,000 units iv). After a median sternotomy, the blood was extracted via the LV apex of a blood supplier rat. This blood was used for priming the cross-circulation tubing. The bilateral common carotid arteries and right external jugular vein of the metabolic supporter rat were cannulated and connected to the arterial and venous cross-circulation tubing, respectively. The anesthetic level of the metabolic supporter rat was maintained at a constant level via additional continuous infusion of pentobarbital sodium at 7.5 mg $h^{-1}$ by monitoring the systemic arterial pressure and heart rate. Consequently, the anesthetic level of the donor heart was constantly maintained. The brachiocephalic artery was cannulated and then the right ventricle (RV) was cannulated via the superior vena cava in the heart donor rat and both the cannulas were connected to the arterial and venous cross-circulation tubing from the supporter rat. The beating heart supported by cross-circulation was then excised from the chest of the heart donor rat [24]. Coronary perfusion of the excised heart was never interrupted during this preparation and the excised heart was maintained at 36°C.

A thin latex balloon (balloon material volume, 0.08 ml) was inserted into the LV via the left atrium and connected to a pressure transducer (Life Kit DX-312, Nihon Kohden, Tokyo, Japan) and a 0.5-ml precision glass syringe with fine scales (minimum scale: 0.005 ml). LV volume (LVV) was changed by adjusting the intra-balloon water volume with the syringe in 0.025-ml steps between 0.08 ml and 0.23 ml (Fig. 2A-1).

Systolic unstressed volume ($V_0$) was determined by filling the balloon to the level where peak isovolumic pressure, and hence pressure-volume area (PVA; see *Data Analysis*), was zero. The sum of the intraballoon water volume and balloon material volume was used as an initial estimate

of $V_0$. $V_0$ was then finally determined as the volume-axis intercept of the best-fit end-systolic pressure (ESP)-volume relation (ESPVR). We obtained the best-fit ESPVR with the equation $ESP=A\{1—\exp[—B(V—V_0)]\}$ by means of the least-squares method (Delta-Graph, DeltaPoint; Monterey, CA) on a personal computer. We also obtained the best-fit end-diastolic pressure (EDP)-volume relation (EDPVR) with the equation $EDP=A'\{\exp[B'(V—V_0')]—1\}$. The correlation coefficients of the best-fit ESPVRs were higher than 0.98.

The heart rate was constantly maintained by electrical pacing of the right atrium at 240 beats per minute (bpm), and the epicardial electrocardiogram was recorded. In our previous study using the ISO-induced hypertrophied model, pacing at 300 bpm caused LV incomplete relaxation [21]. This causes myocardial ischemia and generates lactate. In the present cross-circulation system, oxidative phosphorylation exclusively generates ATP using oxygen, and thus, we measured myocardial oxygen consumption. PVA can accurately express mechanical work when LV complete relaxation occurs. When this is not the case, PVA would be underestimated. The systemic arterial blood pressure of the supporter rat served as the coronary perfusion pressure (90—130 mmHg). Arterial pH, $PO_2$, and $PCO_2$ of the supporter rat were maintained within their physiological ranges with supplemental $O_2$ and sodium bicarbonate.

*2.4. Oxygen consumption*

Myocardial $O_2$ consumption was obtained as the product of coronary flow and coronary arteriovenous $O_2$ content difference ($AVO_2D$). It was divided by pacing rate to obtain $O_2$ consumption per beat ($VO_2$). Total coronary blood flow was continuously measured with an electromagnetic flowmeter (MFV-3100, Nihon Kohden, Tokyo, Japan) placed in the middle of the venous drainage tubing from the RV. The LV thebesian flow was negligible. The coronary $AVO_2D$ was continuously measured by passing all the arterial and venous cross-circulation blood through the cuvettes of a custom-made oximeter (PWA-200S, Shoe Technica; Chiba, Japan) as previously reported in detail [25, 26](Fig. 3A-1). The mean concentration of hemoglobin in the perfused blood was $10.5 \pm 0.9$ mg $dl^{-1}$.

*2.5. Data analysis*

We attempted to fit experimentally obtained LV pressure-volume data to the exponential equations to describe ESPVR and EDPVR. PVA was defined as the area circumscribed by the

curvilinear best-fit ESPVR, EDPVR, and the systolic portions of the ventricular P-V trajectories. PVA was normalized by LV mass to 1 g. On the basis of our previous work with *in vitro* and *in situ* rat hearts, we calculated the mean ESP at midrange LV volume (mLVV)($ESP_{mLVV}$) and PVA at mLVV ($PVA_{mLVV}$) to assess LV mechanical work and energetics [19].

As shown previously [19, 21], the $VO_2$-PVA relationship was linear in the rat LV. Its slope represents the $O_2$ cost of PVA, and its $VO_2$ intercept represents the PVA-independent $VO_2$. The PVA-dependent $VO_2$ is consumed by myosin ATPase for cross-bridge cycling. The PVA-independent $VO_2$ is composed of $O_2$ consumption for $Ca^{2+}$ handling in excitation-contraction (E-C) coupling and basal metabolism. The RV was kept collapsed by continuous hydrostatic drainage so that the RV PVA, and hence PVA-dependent $VO_2$, were assumed to be negligible [25, 26]. The RV component of PVA-independent $VO_2$ was subtracted from the total $VO_2$ to yield LV $VO_2$. The LV (including the septum) and the RV were weighed for normalization of LVV. These data are summarized in Table 1.

*2.6. Experiment protocols*

When we changed LVV by adjusting the intra-balloon water volume with the syringe between 0 ml and 0.23 ml (more than 5 different volumes), LV pressure (LVP), $VO_2$ and PVA data during isovolumic contractions were simultaneously obtained at each LV volume (volume-loading run: vol-run)(Figs. 2A-1 and 3A-1). After the vol-run, a $Ca^{2+}$-induced inotropic run ($Ca^{2+}$ ino-run) was performed at mLVV (0.16 ml = 0.08 ml [$V_0$] plus 0.08 ml [a half value between the minimum and maximum water volume infused into the balloon]) by intracoronary infusion of 1% $CaCl_2$ solution. The infusion rate of $Ca^{2+}$ was increased gradually until we observed a decrease in ESP or arrhythmia due to $Ca^{2+}$ overload. To obtain steady-state data, every data point was measured 3 min after changing the LVV or infusion rate of $Ca^{2+}$.

Finally, to measure the basal metabolic $O_2$ consumption, cardiac arrest was induced by intracoronary infusion of KCl (0.5 M) at 5—10 ml $h^{-1}$ as previously reported [18]. All data were measured and sampled at 1 kHz for 5—10 s and averaged using a PowerLab unit and Chart software (AD Instruments, Bella Vista, NSW, Australia).

*2.7. Oxygen cost of LV contractility*

We obtained the specific best-fit curve for the ESP at $V_0$ (0 mmHg) and the observed $ESP_{mLVV}$

with the best-fit ESPVR function in the control vol-run by the least squares method, and we calculated $PVA_{mLVV}$ during $Ca^{2+}$ infusion using this specific best-fit curve function on a personal computer as previously reported [26]. The $VO_2$-PVA linear relation during $Ca^{2+}$ infusion was shifted upward in parallel with the control $VO_2$-PVA relation. Based on this parallelism, the lines of $VO_2$-PVA linear relationships at different $Ca^{2+}$ infusion rates at mLVV were drawn in parallel to the control $VO_2$-PVA relation line as described previously [25, 27]. The gradually increased $VO_2$-intercept values (PVA-independent $VO_2$ values) of the lines proportional to the enhanced LV contractility by $Ca^{2+}$ were obtained by this procedure. Our proposed index for LV contractility, equivalent maximal elastance at mLVV ($eEmax_{mLVV}$), was calculated from a triangular area equivalent to $PVA_{mLVV}$ [19, 26]. The $O_2$ cost of LV contractility was the slope of the relationship between PVA-independent $VO_2$ and $eEmax_{mLVV}$ (i.e., $VO_2$ used for $Ca^{2+}$ handling in E-C coupling per unit changes in LV contractility).

*2.8. Analyses of one-beat LV pressure-time curve by single logistic function*

To evaluate the LV end-diastolic relaxation rate or lusitropy, we analyzed the logistic time constant ($T_L$) from the respective best-fit functions to a one-beat LV pressure-time curve at mLVV during relaxation with our proposed single logistic function [28, 29].

*2.9. Real-time quantitative reverse transcription (RT)-polymerase chain reaction (PCR)*

The messenger RNA (mRNA) expression levels of SERCA2a, mitochondrial transcription factors A (TFAM) and B2 (TFB2M), and glyceraldehyde-3-phosphate dehydrogenase (GAPDH) were determined by RT-PCR as previously described [22]. RT-PCR was performed using SYBR Green technology on a StepOnePlus™ (Applied Biosystems, Foster City, CA). Total RNA was isolated from frozen tissue samples by a spin protocol using the SV Total RNA Isolation System (Promega, Madison, WI). Complementary DNA (cDNA) was synthesized from 0.5 μg of the total RNA using a ReverTra Ace® qPCR RT kit (Toyobo, Osaka, Japan). The cDNA was initially denatured at 95°C for 30 s and then amplified by PCR for 40 cycles (denaturation at 95°C for 10 s, annealing at 55°C for 10 s, and extension at 72°C for 45 s) using Thunderbird™ SYBR® qPCR Mix (Toyobo). The results were normalized to GAPDH expression.

*2.10. Polyacrylamide gel electrophoresis and western blots for SERCA2a, phospholamban (PLB), phospho-Ser$^{16}$PLB (p-PLB), $Na^+/Ca^{2+}$ exchanger1(NCX1), and TFAM*

Membrane proteins were isolated from the LV wall of each frozen heart. The frozen hearts were homogenized and centrifuged at 1,000 × g for 10 min. The supernatants were centrifuged at 100,000 × g for 60 min at 4°C. The 100,000 × g pellets were cellular membrane fractions and were used for the immunoblotting of SERCA2a, monomeric PLB, p-PLB, NCX1, and TFAM [21, 22].

Equal amounts of the membrane proteins (10 μg $lane^{-1}$) were separated on SDS-polyacrylamide gels (10% for SERCA2; 15% for PLB, p-PLB, and TFAM) in a minigel apparatus (Mini-PROTEAN II, Bio-Rad) and transferred to polyvinyliodene difluoride membranes. The membranes were blocked (4% Block Ace, Dainippon Pharmaceutical Co., Osaka, Japan) and then incubated with anti-SERCA2a antibody (1:1000 dilution; Affinity Bio Reagents, Golden, CO), anti-PLB antibody (1:2000 dilution; Upstate Biotechnology, Lake Placid, NY), anti-p-PLB ($Ser^{16}$) antibody (1:1000 dilution; Upstate Biotechnology), anti-NCX1 antibody (1:200 dilution; a generous gift from Dr. Iwamoto, Fukuoka University), and anti-TFAM antibody (1:1000 dilution; Cell Signaling Technology, Danvers, MA). The antigens were detected by the luminescence method (ECL Western blotting detection kit, GE Healthcare UK Ltd., Amersham Place, Little Chalfont, England) with peroxidase-linked anti-mouse IgG (1:2000 dilution) or peroxidase-linked anti-rabbit IgG (1:2000 or 1:5000 dilution). The amounts of membrane proteins were determined to obtain the linear response of the ECL-immunoblot. After immunoblotting, the film was scanned, and the intensity of the bands was calculated by NIH image analysis [18, 21]. The protein ratio of SERCA2a/PLB, p-PLB/PLB and TFAM/NCX1 for each sample was expressed as a proportion of the mean value obtained for the WT control.

*2.11. Histological analysis*

The hearts of all rats in the WT and TG groups were excised and fixed with 3.7% paraformaldehyde in phosphate-buffered saline, embedded in paraffin, cut into 6-μm slices, and stained with Masson's trichrome (MT) to detect the fibrosis. The LV collagen volume fraction was calculated by counting the computerized pixels in a digital image of the collagen area stained by MT.

*2.12. Statistics*

Multiple comparisons were performed by one-way analysis of variance (ANOVA) with post-hoc Tukey's test, Bonferroni's test, or Games-Howell's test. A value of $P < 0.05$ was

considered statistically significant. All data are expressed as the mean ± S.D.

## 3. Results

### *3.1. Body weights and heart weights*

Body weights (BW) and RV weights (RVW) did not significantly differ among all the WT and TG rat groups. The ratios of heart weight (HW) to BW (HW/BW) in the ISO1w and ISO4w groups were significantly ($P < 0.05$) larger than those of the controls in both the WT and TG rats. In addition, the ratios of LV weights (LVW) to BW (LVW/BW) were significantly ($P < 0.05$) larger in the ISO1w and ISO4w groups than in the WT-control, which indicated ISO-induced cardiac hypertrophy. The ratio of LVW/BW in the TG-ISO4w group was significantly ($P < 0.05$) smaller than that in the TG-ISO1w group but not significantly different from that in the TG-control and WT-ISO4w groups, indicating a partial protection from hypertrophy in the TG-ISO4w group (Table 1).

The summarized data of heart rate (HR) and blood pressure are shown in Table 2. The HR of ISO1w and ISO4w were significantly lower than that of control in both WT and TG, indicating that ISO decreased HR. Systolic blood pressure (SBP), mean blood pressure (MBP), and diastolic blood pressure (DBP) were significantly higher in the TG-ISO4w group than in the others, but not significantly different from those in WT-ISO4w. This result suggests the possibility that the significantly higher *in vivo* SBP and DBP in the TG-ISO4w group are not related to the overexpression of SERCA2a but are instead related to other unknown factors.

### *3.2. Echocardiography*

Summarized echocardiographic data are shown in Figure 1. The functional parameters, LVIDd, and LVIDs of the WT-ISO4w group were significantly ($P < 0.05$) higher than those of the WT-ISO1w group, whereas those of the TG-ISO4w group were not further increased from those of the TG-ISO1w group (Fig. 1A, B), indicating a partial improvement of LV dysfunction in the TG rats.

The wall thickness parameters, IVSTd and LVPWTd, of the ISO1w and ISO4w in WT and TG groups were significantly ($P < 0.05$) larger than those of each control group. The IVSTd —but not LVPWTd—was significantly ($P < 0.05$) lower in the ISO4w group than that in those of the ISO1w

WT and TG groups (Fig. 1C, D). Hence, it is uncertain whether the β-adrenergic receptor inducing cardiac hypertrophy was down-regulated between ISO1w and ISO4w.

Two other functional parameters, EF and FS, were significantly decreased in the ISO4w group compared with the ISO1w group in WT, but not in TG (Fig. 1E, F), which indicates a partial improvement of LV dysfunction in the TG rats.

*3.3. LV mechanical work*

Representative ESPVRs and EDPVRs for all WT and TG rat groups are shown in Figure 2A. The ESPVR of the WT-ISO4w group (blue solid curve in Fig. 2A) was shifted downward compared to the other groups. The ESPVR of the TG-ISO4w group (blue dashed curve in Fig. 2A) was not shifted compared to the other groups. Summarized data of LV mechanics are shown in Table 3. The mean $ESP_{mLVV}$ and $PVA_{mLVV}$ of the WT-ISO4w group were significantly ($P < 0.05$) lower than those of the WT-control group, but the mean $ESP_{mLVV}$ and $PVA_{mLVV}$ of the TG-ISO4w group were not decreased from those of the TG-control group. The mean percentages of $ESP_{mLVV}$ and $PVA_{mLVV}$ normalized to control (=100%) were significantly ($P < 0.05$) smaller in the WT-ISO4w group (Figure 2B and 2C) but not in the TG-ISO4w group. Moreover, the mean percentage of $PVA_{mLVV}$ was significantly ($P < 0.05$) larger in the TG-ISO4w group than in the WT-ISO4w group (Figure 2C). In the ISO4w group, mechanical work was improved by TG.

*3.4. $VO_2$-PVA relations*

Figure 3A shows each representative $VO_2$-PVA relation in all groups, as obtained by the LV volume loading protocol (Fig. 3A-1). All of the $VO_2$-PVA relations could be superimposed. Hence, there were no significant differences in the mean slopes and $VO_2$ intercepts of $VO_2$-PVA relations and, thus, no significant differences in $O_2$ consumptions per minute for basal metabolism and E-C coupling among all groups (Fig. 3B-E).

*3.5. Oxygen cost of LV contractility*

Figure 4A shows that the representative PVA-independent $VO_2$ and $eEmax_{mLVV}$ relations in all groups are linear. The slope of the relation appeared to be lower in the TG-ISO4w group than in the other groups. The slope is defined as the $O_2$ costs of LV contractility: $VO_2$ used for $Ca^{2+}$ handling in E-C coupling per unit change in LV contractility. The mean $O_2$ cost of LV contractility in the TG-ISO4w group was significantly ($P < 0.05$) smaller than those in the other groups (Fig.

4B).

*3.6. Logistic time constant ($T_L$)*

Figure 5A and B show LV pressure-time curves at mLVV normalized to peak pressure in the WT and TG groups, respectively. The normalized systolic LV pressure-time curves could be superimposed. We obtained $T_L$ from each end-diastolic pressure-time curve. The mean $T_L$ of ISO1w and ISO4w were significantly ($P < 0.05$) larger than that the WT control groups (Fig. 5C). The mean $T_L$ was significantly ($P<0.05$) smaller in all TG groups than in the WT-ISO1w and WT-ISO4w groups (Fig. 5C). Each representative raw LV pressure-time curve at mLVV in the WT and TG groups showed a similar systolic pressure-time curve, although the LV peak pressure differed between the groups (Fig. 5D).

*3.7. Western blots for SERCA2a, PLB, p-PLB, and NCX1*

Figure 6A shows representative immunoblotting of SERCA2a, PLB, p-PLB, and NCX1 in each WT and TG group. The mean fold change in the SERCA2a/PLB ratio in the TG-control group was significantly ($P < 0.05$) increased compared to that in the WT-control group (Fig. 6B). Although the mean fold change in SERCA2a/PLB ratio gradually decreased in each WT and TG group over the ISO infusion period, the level in the TG-ISO4w group was significantly ($P < 0.05$) higher than that in the WT-ISO4w group and was maintained at the level of the WT-control group (Fig. 6B). The protein expressions of PLB and p-PLB gradually decreased over the ISO infusion period in the WT and TG groups in a similar manner, and hence, there were no differences in the mean fold change in the p-PLB/PLB ratio among all groups (Fig. 6C). The protein level of NCX1 was not significantly different among all the groups (Fig. 6D).

*3.8. RT-PCR for mRNA of SERCA2a, TFAM, and TFB2M in comparison with GAPDH*

The expression level of each mRNA of SERCA2a, TFAM, and TFB2M in comparison with GAPDH in the WT group was unchanged (Fig. 7A-C). In contrast, the mean expression levels of SERCA2a mRNA in all TG groups were significantly ($P < 0.05$) higher than those in all WT groups (Fig. 7A). The mean expression level of each mRNA of TFAM and TFB2M in all TG groups tended to increase but not significantly (Fig. 7B, C).

*3.9. Western blots for TFAM*

Figure 7D shows representative immunoblotting of TFAM in each WT and TG group. The

mean ratio of TFAM/NCX1 protein expression in the WT group was not significantly different. In contrast, the mean ratios of TFAM/NCX1 protein expression in all TG groups were significantly ($P < 0.05$) higher than that of the WT-ISO1w and WT-ISO4w groups (Fig. 7D).

*3.10. Fibrosis analysis*

The ratio of fibrotic area to whole tissue area in LV was significantly ($P < 0.05$) increased in the ISO1w and ISO4w groups compared with that in the WT and TG control groups, but no differences were found between the ISO1w and ISO4w groups or between the WT and TG groups (Fig. 8).

## 4. Discussion

The present study revealed that (1) LV systolic function was altered in the WT-ISO4w group but was preserved in the TG-ISO4w by analyzing ESPVR, $ESP_{mLVV}$, and $PVA_{mLVV}$ and that (2) LV diastolic function was altered in the WT-ISO1w and WT-ISO4w groups but was preserved in the TG-ISO1w and TG-ISO4w groups by analyzing the logistic time constant. Furthermore, the mean slope and mean $VO_2$ intercept of the $VO_2$-PVA relationships in each of the 6 groups were unchanged under 240-bpm pacing, which is consistent with our previous study [21]. This result indicated that the mean oxygen consumption for $Ca^{2+}$ handling in E-C coupling per minute and the mean oxygen consumption for basal metabolism per minute did not differ among all the groups.

The most interesting finding in the present study was the smaller $O_2$ cost of LV contractility in the ISO4w group than in the control and ISO1w TG groups, although the $O_2$ costs of LV contractility in WT rats were not different among the control, ISO1w, and ISO4w groups.

*4.1. LV mechanical function*

We have previously reported a detailed analysis of a short-term ISO-induced hypertrophy model in WT rats [21]. Although these model hearts showed significant decreases of SERCA2a expression, they were in a compensatory phase, and hence, their LV mechanical work and energetics (except diastolic dysfunction) were unchanged compared with normal WT rats at 240-bpm pacing [21]. In the present study, we made short-term and long-term ISO-infused models. Although we have already reported longer-term ISO-infused models, the cardiac performance was evaluated only by echocardiography [20]. The present study is the first to analyze the detailed

mechanoenergetics of long-term ISO-infused models.

The ESPVR was unchanged in the WT-ISO1w group but shifted downward in the WT-ISO4w group. Thus, decreases in mean $ESP_{mLVV}$ and $PVA_{mLVV}$ were demonstrated in the WT-ISO4w group, indicating systolic dysfunction. The normal systolic function in the WT-ISO1w group was consistent with our previous study [20]. The significantly longer mean $T_L$ of the WT-ISO1w and WT-ISO4w groups indicated diastolic dysfunction. Taken together, the initial LV diastolic dysfunction without systolic dysfunction and the subsequent LV systolic and diastolic dysfunction presented here is similar to the disease progression of concentric LV hypertrophy in human [1].

The systolic and diastolic function could be impaired by the deterioration of $Ca^{2+}$ handling [2, 3]. SERCA2a plays a key role in the $Ca^{2+}$ handling of E-C coupling [2]. The ratio of SERCA2a/PLB in the TG-ISO4w group was maintained at the same level as that of the WT-control group. Therefore, TG-ISO4w could be prevented from impairing the systolic and diastolic function.

*4.2. Smaller $O_2$ cost of LV contractility in TG-ISO4w*

Recently, Pinz et al. demonstrated that overexpression of SERCA2a enhances myocardial mechanical function in a normal model during inotropic stimulation, but that this advantage is not maintained in an LV hypertrophy model in which the energetic status is compromised [16]. They also suggested the possibility that energy supply might be a limiting factor for the benefit of SERCA overexpression in hypertrophied hearts [16]. In the present study, this possibility could be excluded because the lactate production indicating ischemia was not observed in the TG-ISO4w group (data not shown). The smaller $O_2$ cost of LV contractility in the TG-ISO4w group than in the other groups could not be explained by this mechanism [16].

The functioning of ATPases like SERCA2a is highly dependent on the supply of ATP. Therefore, ATP production is tightly related to $Ca^{2+}$ handling in cardiac function. Watanabe et al. [22] demonstrated that mitochondrial TFAM and TFB2M coordinate to regulate the transcription of genes for mitochondrial enzymes that produce ATP and for SERCA2a, which consumes ATP. In contrast, Niwano et al. [30] reported that after SERCA2 gene transfer into the failing heart, mRNA levels of enzymes contributing to the energy supply in mitochondria recovered to normal level, which led to elevated production of ATP. The present result indicated that the ratio of

TFAM/NCX1 in each TG group was significantly larger than that in the WT-1w and WT-4w groups (see Fig. 7D). Accordingly, ATP production might have increased in the TG group. In the TG-ISO4w group, the ratio of SERCA2a/PLB was maintained at the level of that in the WT-control group, (i.e., it did not increase)(see Fig. 6B). Accordingly, ATP production relatively dominates over ATP consumption only in the TG-ISO4w group. This may contribute to the smaller $O_2$ cost of LV contractility in the TG-ISO4w group (see Fig. 4).

Furthermore, in the present study, we used 240-bpm pacing for the ISO1w and ISO4w hearts due to the relaxation dysfunction. In contrast, the smaller $O_2$ cost of LV contractility has been reported in normal hearts that overexpress SERCA2a 2 to 3 days after the infection with an adenovirus carrying SERCA2a under 300-bpm pacing [12]. The experimental models and conditions used were definitely different from ours, leading to the different outcome.

*4.3. $VO_2$-PVA relation*

Because the ESPVR of the WT-ISO4w group was shifted downward from those of the other groups, each PVA at any LVV decreased. Each $VO_2$ at each LVV decreased proportionally to each PVA. However, the slope and the $VO_2$ intercept of the $VO_2$-PVA relation were almost unchanged among all 6 groups, including WT-ISO4w. The slope of the $VO_2$-PVA relation reflects the ratio of chemomechanical energy transduction efficiency of the contractile machinery [19]. The $VO_2$ intercept represents PVA-independent $VO_2$. This is composed of the oxygen consumption for $Ca^{2+}$ handling in E-C coupling and for basal metabolism [19]. These components were also unchanged in all 6 groups.

Nevertheless, the systolic and diastolic dysfunction observed in the WT-ISO4w group was greatly improved in the TG-ISO4w group, and the beneficial smaller oxygen cost of LV contractility was observed in the TG-ISO4w group.

*4.4. Comparison of ex vivo (in vitro) data with in vivo data*

In the present report, the data from the *in vivo* study are shown in Figure 1 and Table 2. The results obtained from an *in vivo* study are frequently complicated and different from those obtained from an *ex vivo* study [31, 32] because various integrative control mechanisms can function *in vivo*. The result obtained from the *ex vivo* study is relatively simple, but experimental conditions can sometimes be different from those in the *in vivo* study. The present *ex vivo* study gave us

information about mechanical work and energetics, but the *in vivo* study could not give us such information. Integrative studies, both *in vivo* and *ex vivo,* are needed to make the result beneficial for clinical therapy.

*4.5. Functional limitations*

The HW/BW and LV/BW of the TG-ISO4w group were significantly greater than those of the WT-control (ratio: 2.89 vs 2.52 and 2.29 vs 2.02). Furthermore, the HW/BW and LV/BW of the TG-ISO4w group were not significantly different from those of the WT-ISO4w group. It seems likely that the increased expression of SERCA2a did not prevent hypertrophic remodeling.

EF and FS remained significantly depressed in the TG-ISO4w compared to the WT control, although the trend was improved. It seems likely that the increased expression of SERCA2a did not preserve EF or FS with ISO treatment.

The ratios of SERCA2a/PLB in the TG-control and TG-ISO1w groups were significantly higher than in the TG-ISO4w group, but the mechanical parameters ($ESP_{mLVV}$ and $PVA_{mLVV}$) were unchanged. Overexpression of SERCA2a was not simply reflected in mechanical parameters.

*4.7. Conclusion*

The present study indicated that longer-term SERCA2a overexpression improved LV systolic and diastolic dysfunction, in the excised heart, and the $O_2$ cost of LV contractility (i.e., the $VO_2$ used for $Ca^{2+}$ handling in E-C coupling per unit change in LV contractility) in a long-term isoproterenol-induced cardiac failure rat model with a down-regulated SERCA2a level. In conclusion, targeting for SERCA2a may be a potential therapeutic strategy for chronic hypertrophic heart failure.

**Acknowledgments**

This work was supported in part by grants-in-aid NO.22790216 for Scientific Research from the Ministry of Education, Culture, Sports, Science and Technology of Japan. The authors thank for a generous gift of anti-NCX1 antibody to Dr. T. Iwamoto, Fukuoka University, Japan.

**Disclosures**

None

**Author contributions**

Miyako Takaki designed and supervised the present study. Shinichi Mitsuyama, Daisuke Takeshita, Koji Obata and Miyako Takaki conducted experiments and obtained the data. Koji Obata and Guo-Xing Zhang established the transgenic rats. Shinichi Mitsuyama and Miyako Takaki analyzed the data and drafted the manuscript.

**References**

[1] Milani RV, Drazner MH, Lavie CJ, Morin DP, Ventura HO. Progression from concentric left ventricular hypertrophy and normal ejection fraction to left ventricular dysfunction. Am J Cardiol 2011; 108: 992-6.

[2] Bers DM. Calcium fluxes involved in control of cardiac myocyte contraction. Circ Res 2000; 87: 275-81.

[3] Gwathmey JK, Copelas L, MacKinnon R, Schoen FJ, Feldman MD, Grossman W, et al. Abnormal intracellular $Ca^{2+}$ handling in myocardium from patients with end-stage heart failure. Circ Res 1987; 61: 70-6.

[4] Arai M, Matsui H, Periasamy M. Sarcoplasmic reticulum gene expression in cardiac hypertrophy and heart failure. Circ Res 1994; 74: 555-64.

[5] Bers DM, Eisner DA, Valdivia HH Sarcoplasmic reticulum $Ca^{2+}$ and heart failure: roles of diastolic leak and $Ca^{2+}$ transport. Circ Res 2003; 93: 487-90.

[6] Mercadier JJ, Lompré AM, Duc P, Boheler KR, Fraysse JB, Wisnewsky C, et al. Altered sarcoplasmic reticulum $Ca^{2+}$-ATPase gene expression in the human ventricle during end-stage heart failure. J Clin Invest 1990; 85: 305-9.

[7] Baker DL, Hashimoto K, Grupp IL, Ji Y, Reed T, Loukianov E, et al. Targeted overexpression of the SR $Ca^{2+}$-ATPase increases cardiac contractility in transgenic mouse hearts. Circ Res 1998; 83: 1205-14.

[8] del Monte F, Williams E, Lebeche D, Schmidt U, Rosenzweig A, Gwathmey JK, et al. Improvement in survival and cardiac metabolism after gene transfer of sarcoplasmic reticulum $Ca^{2+}$-ATPase in a rat model of heart failure. Circulation 2001; 104: 1424-9.

[9] Giordano FJ, He H, McDounough P, Meyer M, Sayen MR, Dillmann WH. Adenovirus-mediated gene transfer reconstitutes depressed SR $Ca^{2+}$-ATPase levels and shortens prolonged cardiac myocyte $Ca^{2+}$ transient. Circulation 1997; 96: 400-3.

[10] Maier LS, Wahl-Schott C, Horn W, Weichert S, Pagel C, Wagner S, et al. Increased SR $Ca^{2+}$ cycling contributes to improved contractile performance in SERCA2a-overexpressing transgenic rats. Cardiovasc Res 2005; 67: 636-46.

[11] Müller OJ, Lange M, Rattunde H, Lorenzen HP, Müller M, Frey N, et al. Transgenic rat hearts overexpressing SERCA2a show improved contractility under baseline conditions and pressure overload. Cardiovasc Res 2003; 59: 380-9.

[12] Sakata S, Lebeche D, Sakata N, Sakata Y, Chemaly ER, Liang LF, et al. Targeted gene transfer increases contractility and decreases oxygen cost of contractility in normal rat hearts. Am J Physiol Heart Circ Physiol 2007; 292: H2356-63.

[13] Sakata S, Lebeche D, Sakata Y, Sakata N, Chemaly ER, Liang L, et al. Transcoronary gene transfer of SERCA2a increases coronary blood flow and decreases cardiomyocyte size in a type 2 diabetic rat model. Am J Physiol Heart Circ Physiol 2007; 292: H1204-7.

[14] Teucher N, Prestle J, Seidler T, Currie S, Elliott EB, Reynolds DF, et al. Excessive sarcoplasmic/endoplasmic reticulum $Ca^{2+}$-ATPase expression causes increased sarcoplasmic reticulum $Ca^{2+}$ uptake but decreases myocyte shortening. Circulation 2004; 110: 3553-9.

[15] Vetter R, Rehfeld U, Reissfelder C, Weiß W, Wagner KD, Günther J, et al. Transgenic overexpression of the sarcoplasmic reticulum $Ca^{2+}$ ATPase improves reticular $Ca^{2+}$ handling in normal and diabetic rat hearts. FASEB J 2002; 16: 1657-9.

[16] Pinz I, Tian R, Belke D, Swanson E, Dillmann W, Ingwall JS. Compromised myocardial energetics in hypertrophied mouse hearts diminish the beneficial effect of overexpressing SERCA2a. J Biol Chem 2011; 286: 10163-8.

[17] Vetter R, Rehfeld U, Reissfelder C, Fechner H, Seppet E, Kreutz R. Decreased cardiac SERCA2 expression, SR Ca uptake, and contractile function in hypothyroidism are attenuated in SERCA2 overexpressing transgenic rats. Am J Physiol Heart Circ Physiol 2011; 300: H943-50.

[18] Zhang GX, Obata K, Takeshita D, Mitsuyama S, Nakashima T, Kikuta A, et al. Evaluation of left ventricular mechanical work and energetics of normal hearts in SERCA2a transgenic rats. J Physiol Sci 2012; 62: 221-31.

[19] Takaki M. Left ventricular mechanoenergetics in small animals. Jpn J Physiol 2004; 54: 175-207.

[20] Takeshita D, Shimizu J, Kitagawa Y, Yamashita D, Tohne K, Nakajima-Takenaka C, et al. Isoproterenol-induced hypertrophied rat hearts: does short-term treatment correspond to

long-term treatment? J Physiol Sci 2008; 58: 179-88.

[21] Nakajima-Takenaka C, Zhang GX, Obata K, Tohne K, Matsuyoshi H, Nagai Y, et al. Left ventricular function of isoproterenol-induced hypertrophied rat hearts perfused with blood: mechanical work and energetics. Am J Physiol Heart Circ Physiol 2009; 297: H1736-43.

[22] Watanabe A, Arai M, Koitabashi N, Niwano K, Ohyama Y, Yamada Y, et al. Mitochondrial transcription factors TFAM and TFB2M regulate Serca2 gene transcription. Cardiovasc Res 2011; 90: 57-67.

[23] Shibata M, Takeshita D, Obata K, Mitsuyama S, Ito H, Zhang G-X, et al. NHE-1 participates in isoproterenol-induced downregulation of SERCA2a and development of cardiac remodeling in rat hearts. Am J Physiol Heart Circ Physiol 2011; 301: H2154-60.

[24] Yoshikawa Y, Zhang GX, Obata K, Ohga Y, Matsuyoshi H, Taniguchi S, et al. Cardioprotective effects of a novel calpain inhibitor SNJ-1945 for reperfusion injury after cardioplegic cardiac arrest. Am J Physiol Heart Circ Physiol 2010; 298: H643-51.

[25] Hata Y, Sakamoto T, Hosogi S, Ohe T, Suga H, Takaki M. Linear $O_2$ use-pressure-volume area relation from curved end-systolic pressure-volume relation of the blood-perfused rat left ventricle. Jpn J Physiol 1998; 48: 197-204.

[26] Tsuji T, Ohga Y, Yoshikawa Y, Sakata S, Kohzuki H, Misawa H, et al. New index for oxygen cost of contractility from curved end-systolic pressure-volume relations in cross-circulated rat hearts. Jpn J Physiol 1999; 49: 513-20.

[27] Sakata S, Ohga Y, Abe T, Tabayashi N, Kobayashi S, Tsuji T, et al. No dependency of a new index for oxygen cost of left ventricular contractility on heart rates in the blood-perfused excised rat heart. Jpn J Physiol 2001; 51: 177-85.

[28] Matsubara H, Araki J, Takaki M, Nakagawa ST, Suga H. Logistic characterization of left ventricular isovolumic pressure-time curve. Jpn J Physiol 1995; 45: 535-52.

[29] Matsubara H, Takaki M, Yasuhara S, Araki J, Suga H. Logistic time constant of isovolumic relaxation pressure-time curve in the canine left ventricle. Better alternative to exponential time constant. Circulation 1995; 92: 2318-26.

[30] Niwano K, Arai M, Koitabashi N, Watanabe A, Ikeda Y, Miyoshi H, et al. Lentiviral vector-mediated SERCA2 gene transfer protects against heart failure and left ventricular

remodeling after myocardial infarction in rats. Mol Ther 2008; 16: 1026-32.

[31] Huke S, Prasad V, Nieman ML, Nattamai KJ, Grupp IL, Lorenz JN, et al. Altered dose response to β-agonists in SERCA1-expressing hearts ex vivo and in vivo. Am J Physiol Heart Circ Physiol 2002; 283: H958 -66.

[32] O'Donnell JM, Fields A, Xu X, Chowdhury SA, Geenen DL, J Bi. Limited functional and metabolic improvements in hypertrophic and healthy hearts expressing the skeletal muscle isoform of SERCA1 by adenoviral gene transfer in vivo. Am J Physiol Heart Circ Physiol 2008; 295: H2483-94.

**Figure Legends**

**Fig. 1** Echocardiographic parameters

The mean values of LV internal dimensions at diastole (LVIDd)(A) and systole (LVIDs)(B), interventricular septum thickness at diastole (IVSTd)(C), left ventricular (LV) posterior wall thickness at diastole (LVPWTd)(D), ejection fraction (EF)(E) and fractional shortening (FS)(F) in each wild-type (WT; n=9 each) and SERCA2a-transgenic rat group (TG; n=7 each) infused with none (Control; solid column), 1-week (ISO1w; gray column) and 4-week isoproterenol (ISO4w; open column) are shown. *, $P < 0.05$ vs. WT-Control. †, $P < 0.05$ vs. WT-ISO1w. ‡, $P < 0.05$ vs. WT-ISO4w. §, $P < 0.05$ vs. TG-Control. ¶, $P < 0.05$ vs. TG-ISO1w

**Fig. 2** Representative LV end-systolic pressure-volume relations (ESPVRs) and end-diastolic pressure-volume relations (EDPVRs)(A) and mechanical indices (B, C)

A-1: Representative simultaneous tracings of left ventricular (LV) isovolumic pressure and LV volume during volume-loading run between 0.08 ($V_0$) ml and 0.23 ($V_0$ + 0.15) ml. From the data by this protocol, a single set of ESPVR and EDPVR is obtainable.

B: The mean percentage normalized to control (=100%) in end-systolic pressure (ESP) at midrange LV volume (mLVV)(= $ESP_{mLVV}$) in each WT (n=9 each) and TG rat group (n=7 each).

C: The mean percentage normalized to control (=100%) in systolic pressure-volume area (PVA: a total mechanical energy per beat) at mLVV (= $PVA_{mLVV}$) in each WT (n=9 each) and TG rat group (n=7 each). *, $P < 0.05$ vs. WT-Control. ‡, $P < 0.05$ vs. WT-ISO4w.

**Fig. 3** Representative LV oxygen consumption per beat ($VO_2$)-PVA relations (A) and summary of mechanoenergetic indices (B-E)

A-1: Representative simultaneous tracings of left ventricular (LV) isovolumic pressure, mean coronary flow, coronary arteriovenous $O_2$ content difference ($AVO_2D$), and LV volume during volume-loading run bewteen 0.08 ($V_0$) ml and 0.25 ($V_0$ + 0.15) ml. From the data by this protocol, a single $VO_2$-PVA relation is obtainable. The mean slopes (B) and $VO_2$ intercepts (C) of the $VO_2$-PVA relations, and oxygen consumption per minute for basal metabolism (D) and

excitation-contraction (E-C) coupling (E) are shown in each WT (n=9 each) and TG group (n=7 each). There was no significant difference among all groups.

**Fig. 4** Representative PVA-independent $VO_2$-equivalent maximal elastance (eEmax) at mLVV (= $eEmax_{mLVV}$) relations (A) and the mean slopes of the relations (B) in the 6 groups.

The slope of the relation denotes oxygen cost of $eEmax_{mLVV}$ (=LV contractility). The mean oxygen costs of LV contractility are shown in each WT (n=5-6) and TG group (n=5-8). *, $P < 0.05$ vs. WT-Control. †, $P < 0.05$ vs. WT-ISO1w. §, $P < 0.05$ vs. TG-Control. ¶, $P < 0.05$ vs. TG-ISO1w.

**Fig. 5** Representative normalized LV pressure-time curves at mLVV in each WT (A) and TG (B) group and the mean logistic time constants (Matsubara et al., Circulation 1995; 92: 2318-26)(C)

From end-diastolic pressure-time curves within the frame (A, B), we obtained the mean logistic time constants (C) in each WT (n=9 each) and TG group (n=7 each). D: Raw pressure-time curves in each WT and TG group. Raw systolic pressure-time curves were almost superimposable, indicating similar contraction rates. *, $P < 0.05$ vs. WT-Control. †, $P < 0.05$ vs. WT-ISO1w. ‡, $P < 0.05$ vs. WT-ISO4w.

**Fig. 6** Representative immunoblotting (A) and the summary of the mean protein levels of cardiac $Ca^{2+}$ handling proteins (B-D)

The mean ratios of sarcoplasmic reticulum $Ca^{2+}$ATPase (SERCA2a)/phospholamban (PLB) (n=7-11)(B) and the mean ratios of phosphorylated-$Ser^{16}$ PLB (p-PLB)/ PLB (n=5-11)(C) and the mean protein levels of $Na^+/Ca^{2+}$ exchanger 1 (NCX1) (n=8)(D) are shown in each WT and TG group. *, $P < 0.05$ vs. WT-Control. †, $P < 0.05$ vs. WT-ISO1w. ‡, $P < 0.05$ vs. WT-ISO4w. §, $P < 0.05$ vs. TG-Control. ¶, $P < 0.05$ vs. TG-ISO1w

**Fig. 7** RT-PCR for mRNA of SERCA2a (A), mitochondrial transcription factors A (TFAM)(B) and B2 (TFB2M)(C) and western blots for TFAM (D)

RT-PCR for mRNA of SERCA2a, TFAM, and TFB2M was compared with glyceraldehyde-3-phosphate dehydrogenase (GAPDH). TFAM protein level was normalized to NCX1 protein

level. The mean values of RT-PCR and western blots are shown in each WT and TG group (n=5-7 each). †, P < 0.05 vs. WT-ISO1w. ‡, P < 0.05 vs. WT-ISO4w.

Fig. 8 Fibrotic area ratio to whole tissue area in LV in each WT (n= each 6 view in 6 rats) and TG (n= each 6 view in 6 rats) group

The mean fibrotic area ratios in the ISO1w and ISO4w groups were significantly higher compared with those in the control groups. *, P < 0.05 vs. WT-Control. §, P < 0.05 vs. TG-Control.

Figure 1

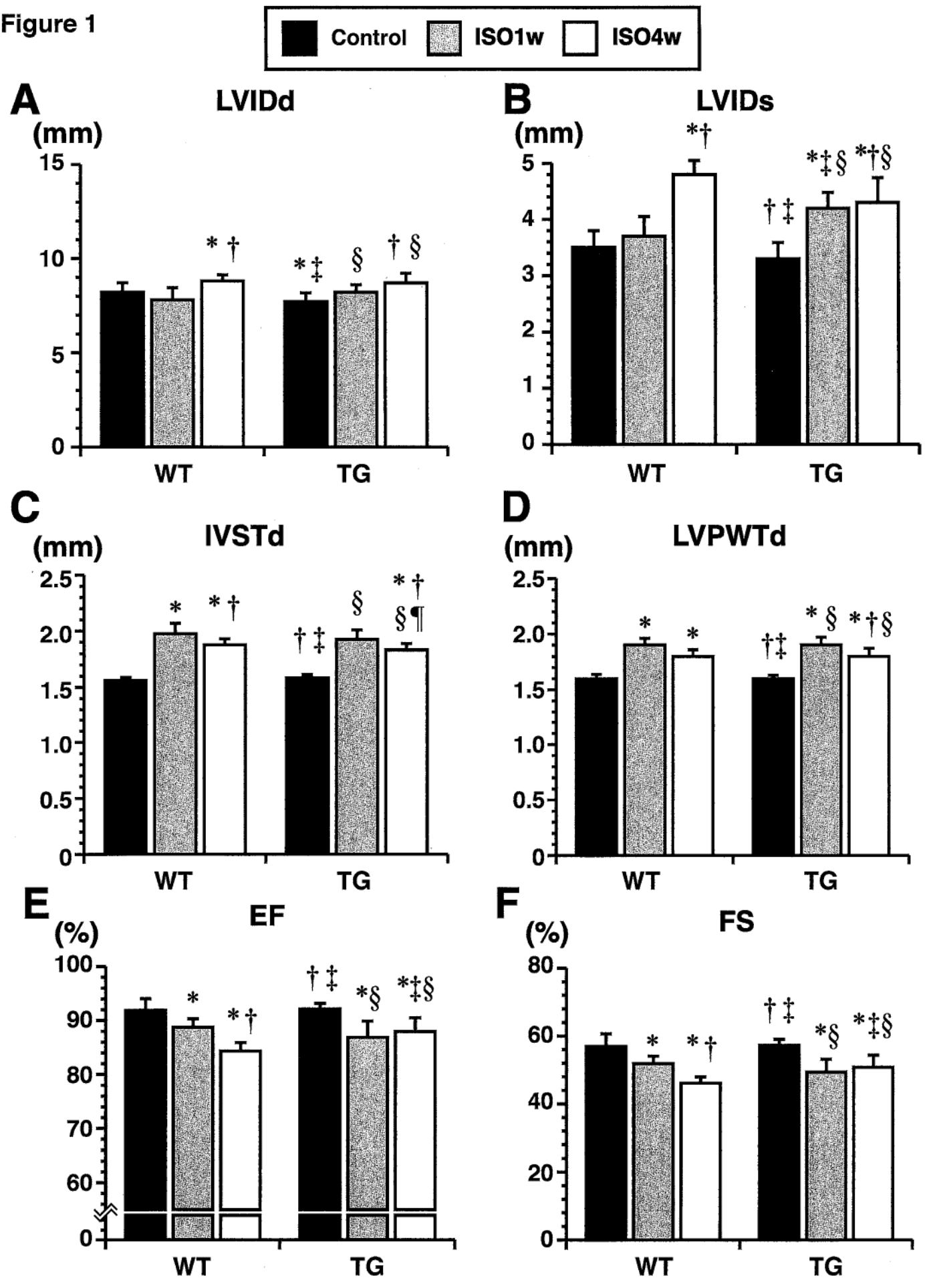
Control
ISO1w
ISO4w
A
LVIDd
(mm)
15
10
5
0
WT
TG
B
LVIDs
(mm)
5
4
3
2
1
0
WT
TG
C
IVSTd
(mm)
2.5
2.0
1.5
1.0
0.5
0
WT
TG
D
LVPWTd
(mm)
2.5
2.0
1.5
1.0
0.5
0
WT
TG
E
EF
(%)
100
90
80
70
60
0
WT
TG
F
FS
(%)
80
60
40
20
0
WT
TG

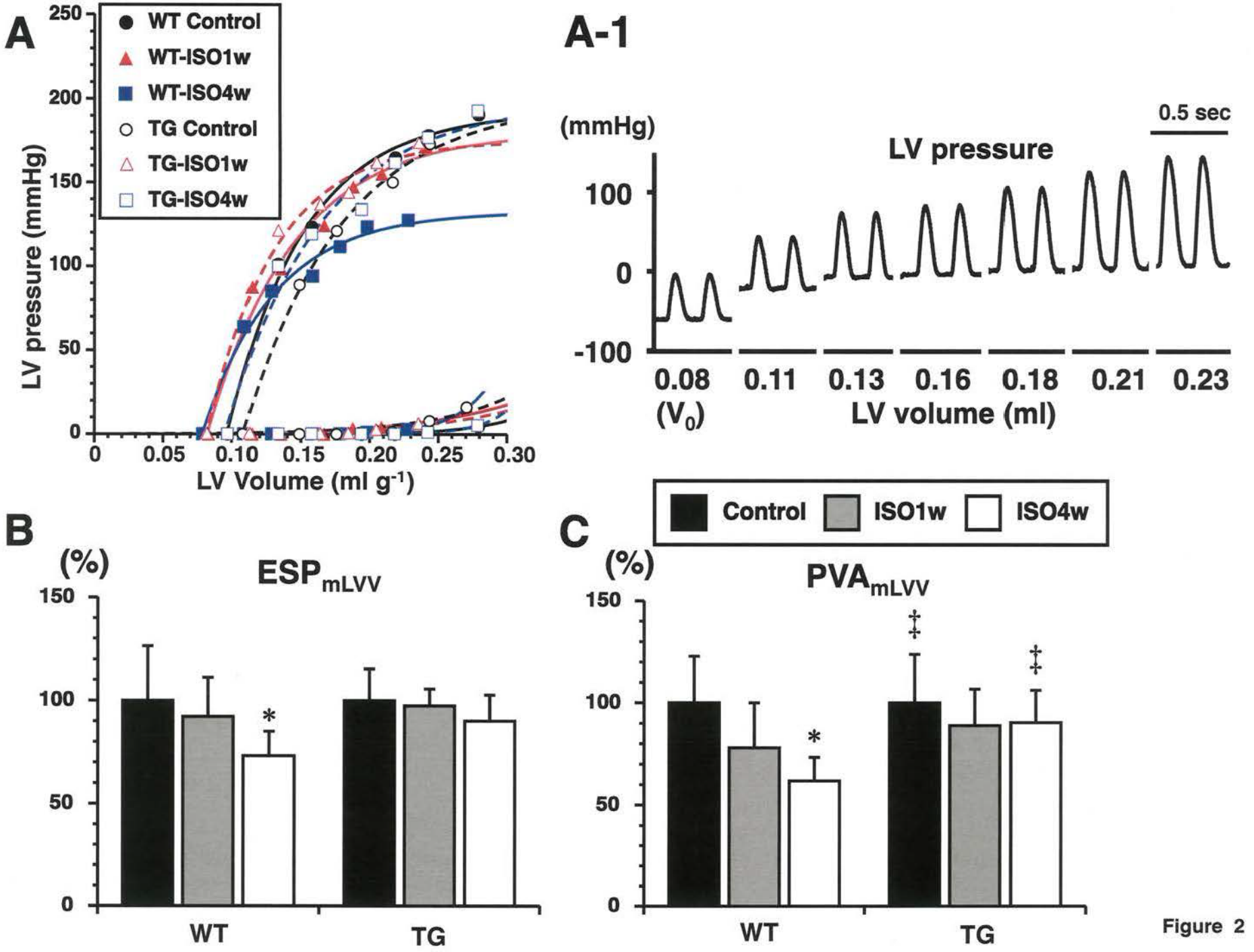
A
WT Control
WT-ISO1w
WT-ISO4w
TG Control
TG-ISO1w
TG-ISO4w
LV pressure (mmHg)
LV Volume (ml g-1)
A-1
(mmHg)
LV pressure
0.5 sec
100
0
-100
0.08
(V0)
0.11
0.13
0.16
0.18
0.21
0.23
LV volume (ml)
B
(%)
ESPmLVV
WT
TG
C
Control
ISO1w
ISO4w
(%)
PVAmLVV
WT
TG

Figure 2

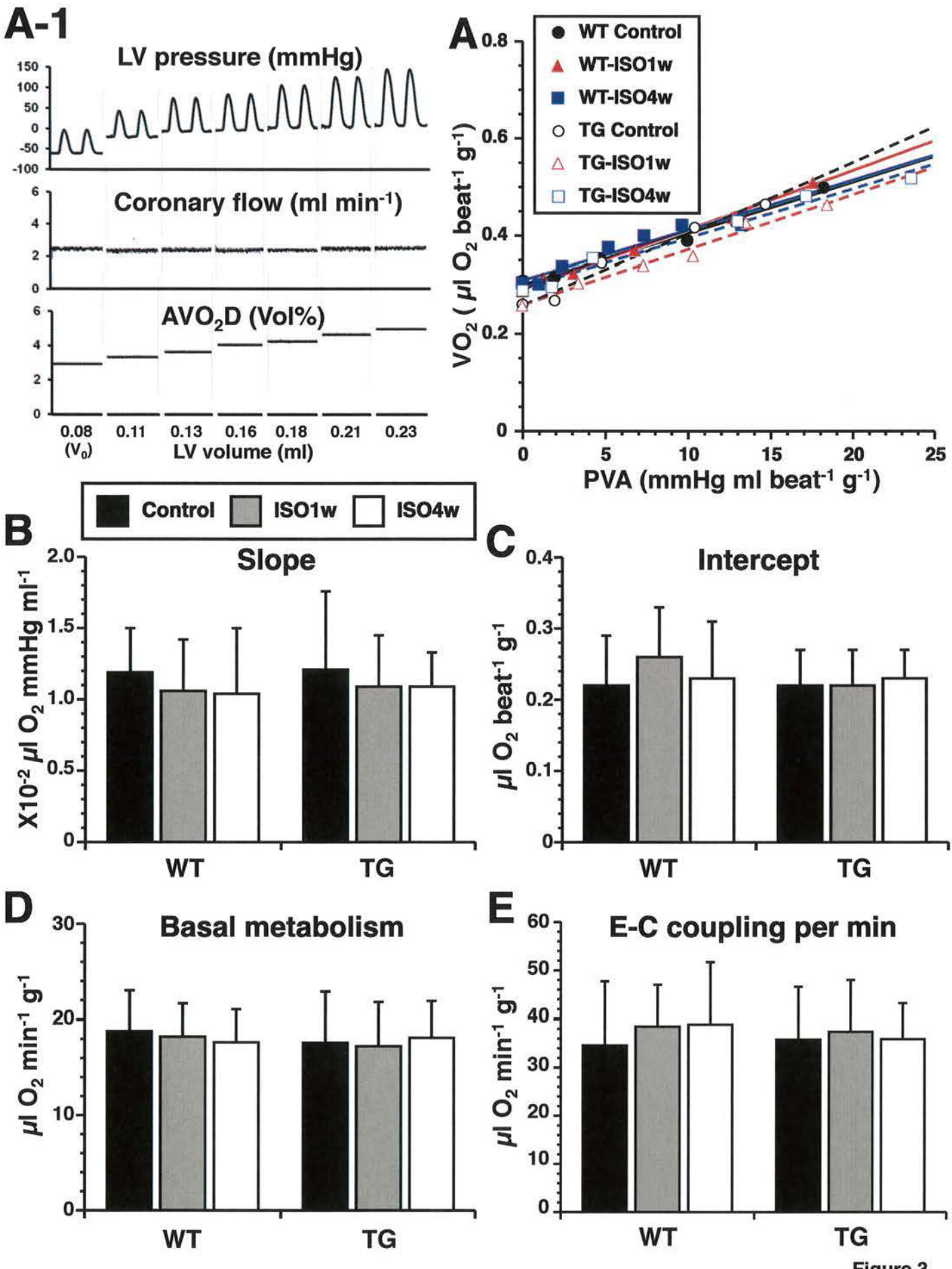
A-1
LV pressure (mmHg)
150
100
50
0
-50
-100
Coronary flow (ml min-1)
6
4
2
0
AVO2D (Vol%)
6
4
2
0
0.08
(V0)
0.11
0.13
0.16
0.18
0.21
0.23
LV volume (ml)
A
WT Control
WT-ISO1w
WT-ISO4w
TG Control
TG-ISO1w
TG-ISO4w
VO2 (μl O2 beat-1 g-1)
0.8
0.6
0.4
0.2
0
0
5
10
15
20
25
PVA (mmHg ml beat-1 g-1)
Control
ISO1w
ISO4w
B
Slope
X10-2 μl O2 mmHg ml-1
2.0
1.5
1.0
0.5
0
WT
TG
C
Intercept
μl O2 beat-1 g-1
0.4
0.3
0.2
0.1
0
WT
TG
D
Basal metabolism
μl O2 min-1 g-1
30
20
10
0
WT
TG
E
E-C coupling per min
μl O2 min-1 g-1
60
50
40
30
20
10
0
WT
TG

Figure 3

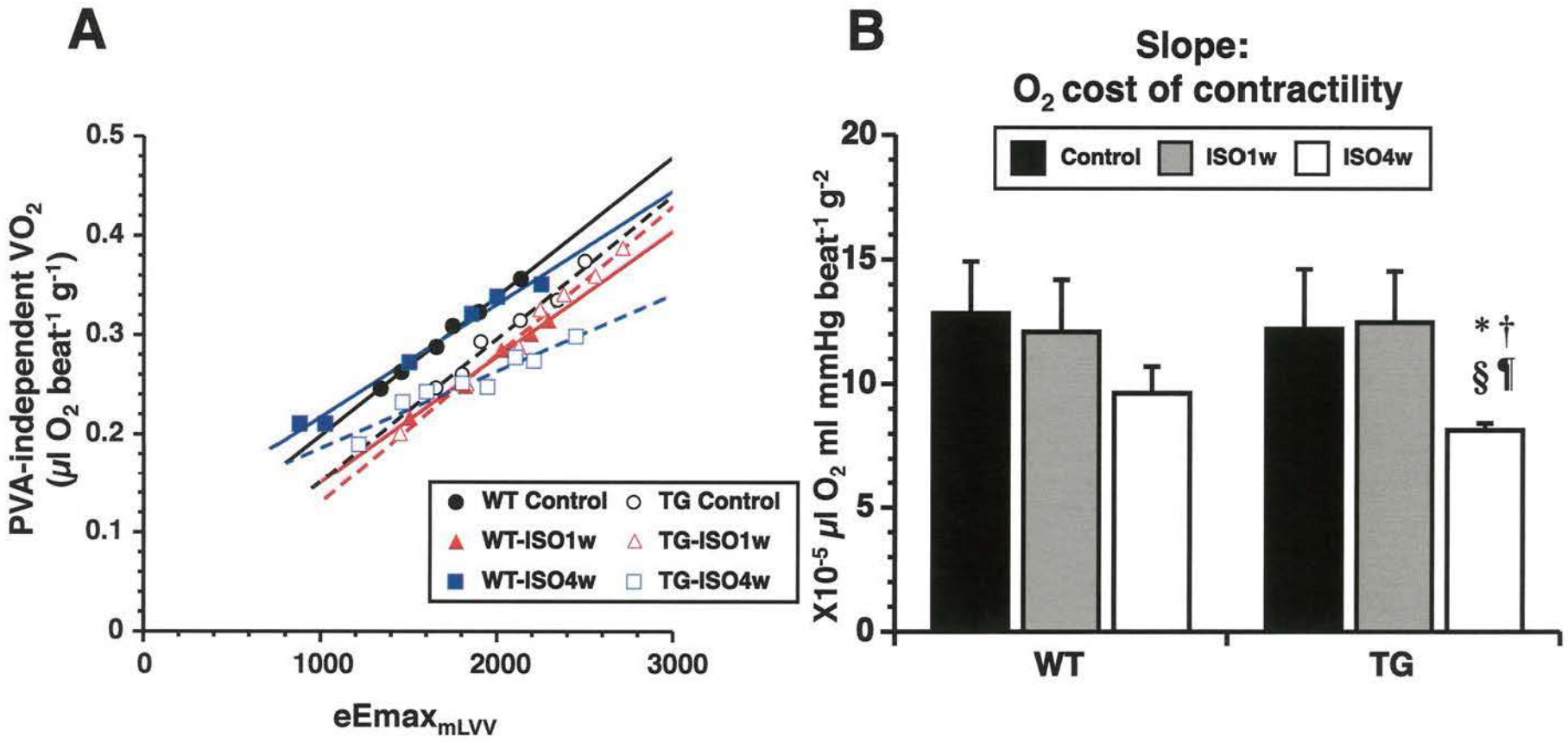
A
PVA-independent $VO_2$ ($\mu l$ $O_2$ $beat^{-1}$ $g^{-1}$)
0.5
0.4
0.3
0.2
0.1
0
0
1000
2000
3000
$eEmax_{mLVV}$
WT Control
TG Control
WT-ISO1w
TG-ISO1w
WT-ISO4w
TG-ISO4w
B
Slope:
$O_2$ cost of contractility
$X10^{-5}$ $\mu l$ $O_2$ ml mmHg $beat^{-1}$ $g^{-2}$
20
15
10
5
0
Control
ISO1w
ISO4w
WT
TG
* †
§ ¶

Figure 4

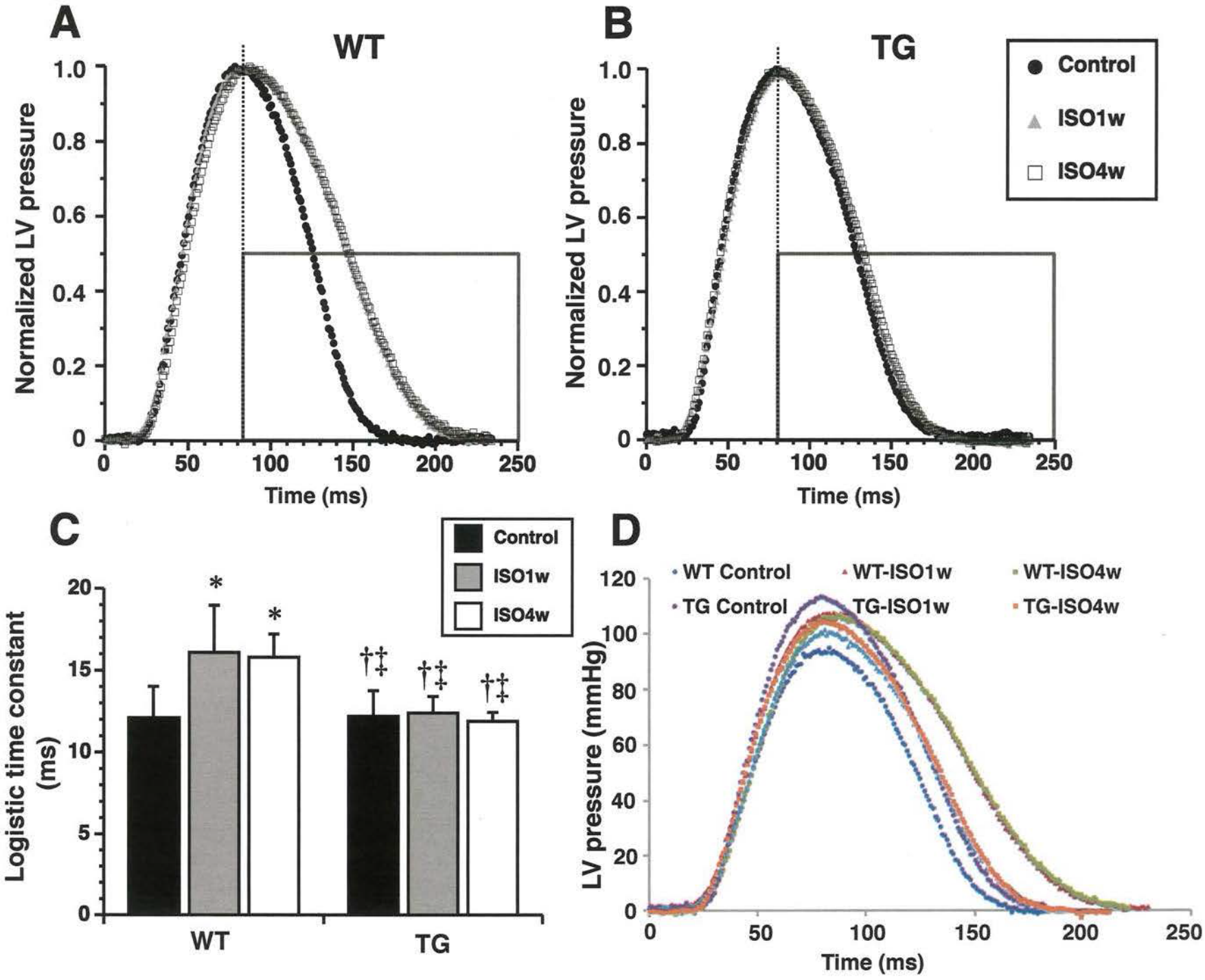
A
WT
Normalized LV pressure
Time (ms)
B
TG
Control
ISO1w
ISO4w
C
Logistic time constant (ms)
WT
TG
D
WT Control
WT-ISO1w
WT-ISO4w
TG Control
TG-ISO1w
TG-ISO4w
LV pressure (mmHg)
Time (ms)

Figure 5

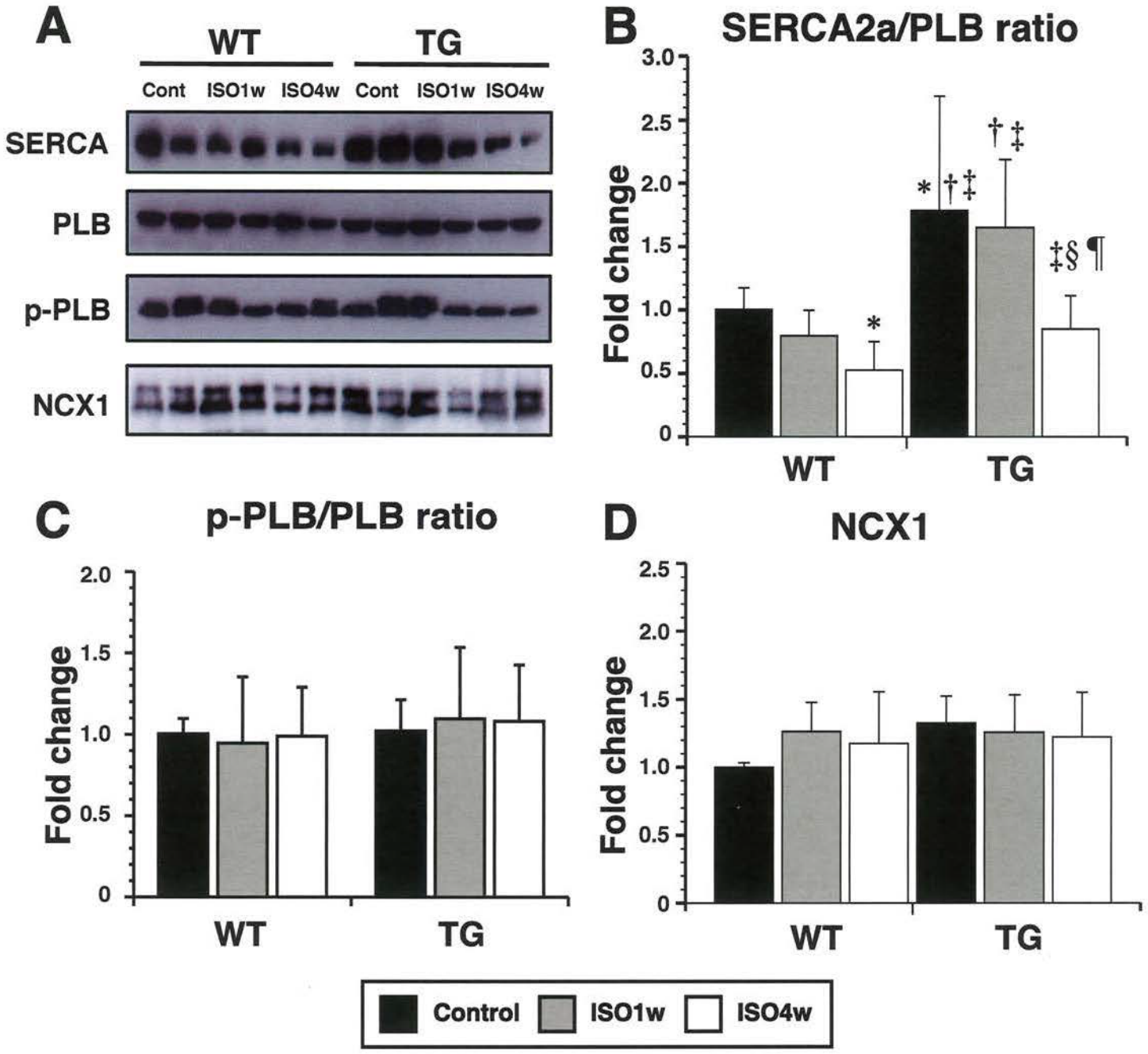
A
WT
TG
Cont
ISO1w
ISO4w
Cont
ISO1w
ISO4w
SERCA
PLB
p-PLB
NCX1
B
SERCA2a/PLB ratio
Fold change
3.0
2.5
2.0
1.5
1.0
0.5
0
*
*†‡
†‡
‡§¶
WT
TG
C
p-PLB/PLB ratio
Fold change
2.0
1.5
1.0
0.5
0
WT
TG
D
NCX1
Fold change
2.5
2.0
1.5
1.0
0.5
0
WT
TG
Control
ISO1w
ISO4w

Figure 6

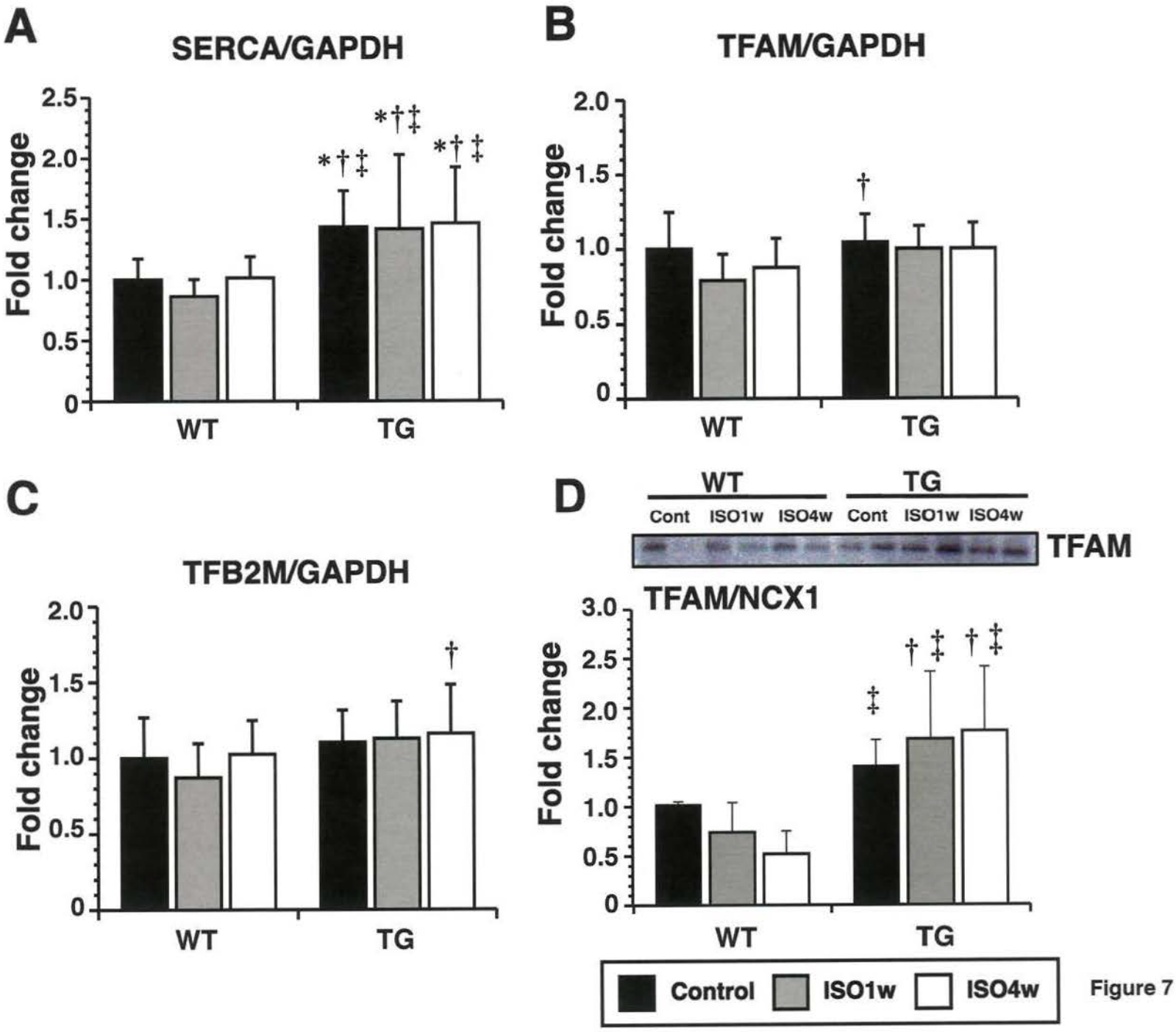
A
SERCA/GAPDH
Fold change
2.5
2.0
1.5
1.0
0.5
0
*†‡
*†‡
*†‡
WT
TG
B
TFAM/GAPDH
Fold change
2.0
1.5
1.0
0.5
0
†
WT
TG
C
TFB2M/GAPDH
Fold change
2.0
1.5
1.0
0.5
0
†
WT
TG
D
WT
TG
Cont
ISO1w
ISO4w
Cont
ISO1w
ISO4w
TFAM
TFAM/NCX1
Fold change
3.0
2.5
2.0
1.5
1.0
0.5
0
‡
† ‡
† ‡
WT
TG
Control
ISO1w
ISO4w

Figure 7

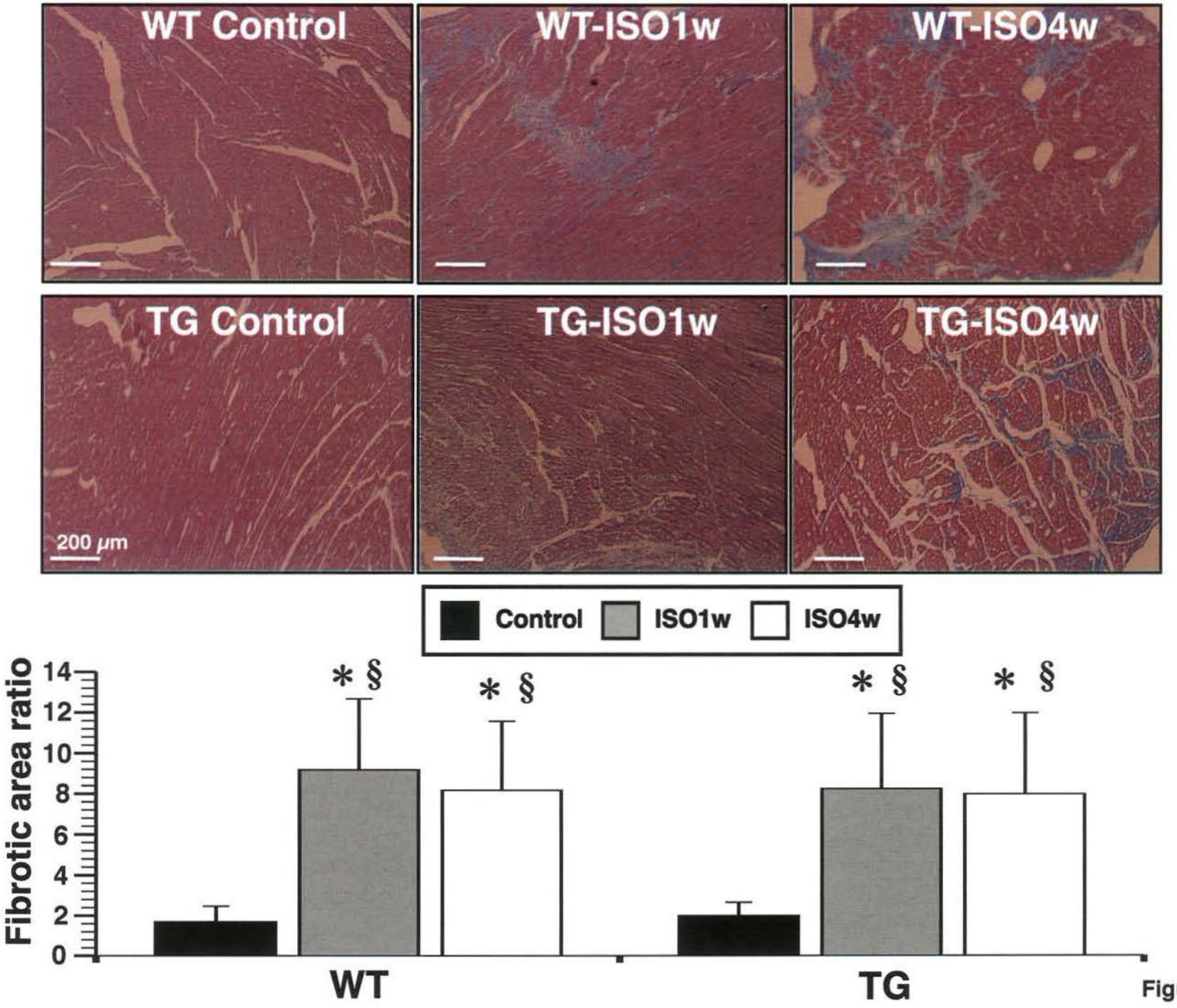
WT Control
WT-ISO1w
WT-ISO4w
TG Control
TG-ISO1w
TG-ISO4w
200 μm
Control
ISO1w
ISO4w
Fibrotic area ratio
0
2
4
6
8
10
12
14
* §
* §
* §
* §
WT
TG

Figure 8

Table 1. Body weights and heart weights

| | WT | | | TG | | |
|---|---|---|---|---|---|---|
| | Control (n=11) | ISO1w (n=9) | ISO4w (n=7) | Control (n=7) | ISO1w (n=7) | ISO4w (n=7) |
| BW (g) | 428 ± 57.2 | 407 ± 35.2 | 415 ± 27.4 | 393 ± 39.6 | 373 ± 19.9 | 395 ± 21.6 |
| LVW (g) | 0.863 ± 0.149 | 0.961 ± 0.086 | 0.988 ± 0.092 | 0.808 ± 0.074‡ | 0.970 ± 0.077 | 0.905 ± 0.065 |
| RVW (g) | 0.218 ± 0.040 | 0.266 ± 0.051 | 0.251 ± 0.046 | 0.207 ± 0.024 | 0.258 ± 0.030 | 0.237 ± 0.032 |
| HW/BW ($X10^{-3}$) | 2.52 ± 0.185 | 3.02 ± 0.152* | 2.99 ± 0.127* | 2.59 ± 0.180†‡ | 3.29 ± 0.124*†‡§ | 2.89 ± 0.115*§ ‖ |
| LVW/BW ($X10^{-3}$) | 2.02 ± 0.187 | 2.37 ± 0.186* | 2.38 ± 0.081* | 2.07 ± 0.157†‡ | 2.60 ± 0.126*§ | 2.29 ± 0.159* ‖ |
| RVW/BW ($X10^{-3}$) | 0.508 ± 0.054 | 0.649 ± 0.082* | 0.605 ± 0.089 | 0.527 ± 0.039† | 0.692 ± 0.062*§ | 0.597 ± 0.062 |

Values are means ± SD; n, number of animals; WT, wild-type rats; TG, SERCA2a-transgenic rats; ISO1w and ISO4w, isoproterenol (1.2 mg $kg^{-1}$ $day^{-1}$ for 1 week or 4 weeks, respectively)-infused group; BW, body weight; LVW, left ventricle weight; RVW, right ventricle weight; HW, heart weight. * $P < 0.05$ vs. WT-Control. †$P < 0.05$ vs. WT-ISO1w. ‡$P < 0.05$ vs. WT-ISO4w. §$P < 0.05$ vs. TG-Control. ‖ $P < 0.05$ vs. TG-ISO1w. All animals treated with ISO for 4 weeks survived.

Table 2. Heart rate and blood pressure

| | WT | | | TG | | |
|---|---|---|---|---|---|---|
| | Control (n=12) | ISO1w (n=9) | ISO4w (n=13) | Control (n=11) | ISO1w (n=10) | ISO4w (n=15) |
| Heart Rate (bpm) | 378 ± 35 | 325 ± 38*§ | 329 ± 26*§ | 403 ± 26 | 347 ± 35§ | 336 ± 37*§ |
| Systolic Blood Pressure (mmHg) | 135 ± 15 | 132 ± 12 | 149 ± 11† | 142 ± 9 | 131 ± 14‡ | 158 ± 13*†§ ‖ |
| Mean Blood Pressure (mmHg) | 116 ± 13 | 115 ± 11 | 125 ± 10 | 120 ± 9 | 114 ± 12 | 137 ± 12*†§ ‖ |
| Diastolic Blood Pressure (mmHg) | 107 ± 13 | 108 ± 10 | 113 ± 11 | 109 ± 9 | 106 ± 12 | 126 ± 13*†§ ‖ |

Values are means ± SD; n, number of animals; WT, wild-type rats; TG, SERCA2a-transgenic rats; ISO1w and ISO4w, isoproterenol (1.2 mg $kg^{-1}$ $day^{-1}$ for 1 week or 4 weeks, respectively)-infused group; bpm, beats per minute; * $P < 0.05$ vs. WT-Control. †$P < 0.05$ vs. WT-ISO1w. ‡$P < 0.05$ vs. WT-ISO4w. §$P < 0.05$ vs. TG-Control. ‖ $P < 0.05$ vs. TG-ISO1w.

Table 3. Variables of left ventricular mechanics

| | WT | | | TG | | |
|---|---|---|---|---|---|---|
| | Control (n=11) | ISO1w (n=9) | ISO4w (n=7) | Control (n=7) | ISO1w (n=7) | ISO4w (n=7) |
| ESPVR | | | | | | |
| A (mmHg) | 212 ± 51.9 | 160 ± 26.4 | 135 ± 21.8* | 265 ± 64.5†‡ | 207 ± 59.7 | 164 ± 21.2§ |
| B ($ml^{-1}$) | 15.0 ± 6.03 | 27.1 ± 9.22* | 21.1 ± 4.60 | 8.90 ± 3.75†‡ | 17.6 ± 7.33 | 19.2 ± 8.90 |
| $V_0$ ($x10^{-2}$ ml $g^{-1}$) | 0.095 ± 0.014 | 0.083 ± 0.007 | 0.081 ± 0.008 | 0.100 ± 0.009†‡ | 0.083 ± 0.007§ | 0.088 ± 0.006 |
| EDPVR | | | | | | |
| A' (mmHg) | 0.124 ± 0.128 | 0.276 ± 0.172 | 0.091 ± 0.071 | 0.214 ± 0.183 | 0.175 ± 0.134 | 0.104 ± 0.100 |
| B' ($ml^{-1}$) | 35.2 ± 14.0 | 35.2 ± 11.2 | 34.1 ± 16.8 | 29.2 ± 9.00 | 35.3 ± 13.4 | 38.1 ± 20.0 |
| $ESP_{mLVV}$ (mmHg) | 139 ± 36.7 | 129 ± 26.5 | 102 ± 16.6* | 132 ± 20.2 | 128 ± 10.8 | 119 ± 16.6 |
| $PVA_{mLVV}$ (mmHg ml $beat^{-1}$ $g^{-1}$) | 9.11 ± 2.09 | 7.11 ± 2.00 | 5.63 ± 1.05* | 8.04 ± 1.92 | 7.15 ± 1.43 | 7.27 ± 1.28 |
| mLVV (ml $g^{-1}$) | 0.190 ± 0.028 | 0.162 ± 0.016* | 0.163 ± 0.015 | 0.199 ± 0.018†‡ | 0.166 ± 0.014§ | 0.178 ± 0.014 |

Values are means ± SD; n, number of animals; WT, wild-type rats; TG, SERCA2a-transgenic rats; ISO1w and ISO4w, isoproterenol (1.2 mg $kg^{-1}$ $day^{-1}$ for 1 week or 4 weeks, respectively)-infused group; ESPVR, end-systolic pressure (ESP)-volume (V) relation; A and B, parameters of best-fit ESPVR obtained by the equation: $ESP=A\{1—\exp[—B(V—V_0)]\}$. Each best-fit curve was obtained by ESP-V data during left ventricular (LV) volume-loading run; $V_0$, volume intercept of ESPVR normalized by LV mass to 1 g; EDPVR, end-diastolic pressure-volume relation; A' and B', parameters of best-fit EDPVR obtained by the equation: $EDP=A'\{\exp[B'(V—V_0')]—1\}$; mLVV, midrange LV volume; $ESP_{mLVV}$, ESP at mLVV; $PVA_{mLVV}$, systolic pressure-volume area at mLVV. * $P < 0.05$ vs. WT-Control. † $P < 0.05$ vs. WT-ISO1w. ‡ $P < 0.05$ vs. WT-ISO4w. § $P < 0.05$ vs. TG-Control.